Synthesis, Crystal Structures, and Properties of Oxovanadium(IV)–Lanthanide(III) Heteronuclear Complexes

Wei Shi,[a] Xiao-Yan Chen,[a] Yan-Nan Zhao,[a] Bin Zhao,[a] Peng Cheng,*[a] Ao Yu,[b] Hai-Bin Song,[c] Hong-Gen Wang,[c] Dai-Zheng Liao,[a] Shi-Ping Yan,[a] and Zong-Hui Jiang[a]

Abstract: A new series of oxovanadium(IV)–lanthanide(III) heteronuclear complexes $[Yb(H_2O)_8]_2[(VO)_2(TTHA)]_3\cdot 21\,H_2O$ (**1**), $\{[Ho(H_2O)_7(VO)_2(TTHA)][(VO)_2(TTHA)]_{0.5}\}\cdot 8.5\,H_2O$ (**2**), $\{[Gd(H_2O)_7(VO)_2(TTHA)][(VO)_2(TTHA)]_{0.5}\}\cdot 8.5\,H_2O$ (**3**), $\{[Eu(H_2O)_7][(VO)_2(TTHA)]_{1.5}\}\cdot 10.5\,H_2O$ (**4**), and $[Pr_2(H_2O)_6(SO_4)_2][(VO)_2(TTHA)]$ (**5**) (H_6TTHA = triethylenetetraaminehexaacetic acid) were prepared by using the bulky flexible organic acid H_6TTHA as structure-directing agent. X-ray crystallographic studies reveal that they contain the same $[(VO)_2(TTHA)]^{2-}$ unit as building block, but the Ln^{3+} ion lies in different coordination environments. Although the lanthanide ions always exhibit similar chemical behavior, the structures of the complexes are not homologous. Compound **1** is composed of a $[Yb(H_2O)_8]^{3+}$ ion and a $[(VO)_2(TTHA)]^{2-}$ ion. Compounds **2** and **3** are isomorphous; both contain a trinuclear $[Ln(H_2O)_7(VO)_2(TTHA)]^{+}$ (Ln = Ho for **2** and Gd for **3**) ion and a $[(VO)_2(TTHA)]^{2-}$ ion. Compound **4** is an extended one-dimensional chain, in which each Eu^{3+} ion links two $[(VO)_2(TTHA)]^{2-}$ ions. For **5**, the structure is further assembled into a three-dimensional network with an interesting framework topology comprising V_2Pr_2 and V_4Pr_2 heterometallic lattices. Moreover, **4** and **5** are the first oxovanadium(IV)–lanthanide(III) coordination polymers and thus enlarge the realm of 3d–4f complexes. The IR, UV/Vis, and EPR spectra and the magnetic properties of the heterometallic complexes were studied. Notably, **2** shows unusual ferromagnetic interactions between the VO^{2+} and Ho^{3+} ions.

Keywords: heterometallic complexes · lanthanides · magnetic properties · N,O ligands · vanadium

Introduction

In recent years, increasing interest has been paid to self-assembled supramolecular compounds because of their exploitable properties such as magnetism, catalysis, molecular sensors, and so on.[1] The artificial construction of transition-metal–lanthanide supramolecular complexes is expected to generate new functional materials due to their optical and magnetic properties. Although a number of structures containing 3d/4f metals solely or 3d–4f discrete complexes has been successfully designed and synthesized, the assembly of extended structures of 3d–4f heteronuclear coordination polymers is still a challenge and of current interest for chemists.[2,3]

The coordination chemistry of the 3d metal vanadium is of interest for applications in the areas of biochemistry, medicine, and catalysis.[4] To the best of our knowledge, reported X-ray structure determinations of vanadium compounds have focused mainly on polyoxovanadates, polyoxovanadate/metal–ligand systems, and mono- or binuclear vanadium complexes,[5] while multidimensional oxovanadium–lanthanide coordination polymers remain elusive.[6] There are various synthetic strategies for the construction of diverse complexes and coordination polymers; for example: choosing appropriate polycarboxylic acids as structure-di-

[a] W. Shi, X.-Y. Chen, Y.-N. Zhao, Dr. B. Zhao, Prof. Dr. P. Cheng, D.-Z. Liao, S.-P. Yan, Z.-H. Jiang
Department of Chemistry, Nankai University
Tianjin 300071 (P.R. China)
Fax: (+86) 22-23502458
E-mail: pcheng@nankai.edu.cn

[b] A. Yu
Central Laboratory, Nankai University
Tianjin 300071 (P.R. China)

[c] Dr. H.-B. Song, H.-G. Wang
State Key Laboratory of Elemento-Organic Chemistry
Nankai University
Tianjin 300071 (P.R. China)

 DOI: 10.1002/chem.200500086

recting agents, adjusting the pH of the reacting system, altering the reaction temperature and pressure, controlling the molar ratio of the raw materials, and changing the atomic size of the metal ions.[7] The lanthanide ions can modulate the structures of some complexes with flexible ligands due to the decreasing atomic size with increasing atomic number, but this phenomenon was not observed for 3d–4f mixed complexes or coordination polymers.[7] We have synthesized a new series of heteronuclear oxovanadium–lanthanide complexes **1**–**5** (H_6TTHA = triethylenetetraaminehexaacetic acid). To the best of our knowledge, the structure of the complexes formed by H_6TTHA and lanthanide ions had not been studied by X-ray diffraction until 1997.[8] Heteronuclear complexes or coordination polymers formed with this ligand remain elusive.

$[Yb(H_2O)_8]_2[(VO)_2(TTHA)]_3 \cdot 21\,H_2O$ **1**

$\{[Ho(H_2O)_7(VO)_2(TTHA)][(VO)_2(TTHA)]_{0.5}\} \cdot 8.5\,H_2O$ **2**

$\{[Gd(H_2O)_7(VO)_2(TTHA)][(VO)_2(TTHA)]_{0.5}\} \cdot 8.5\,H_2O$ **3**

$\{[Eu(H_2O)_7][(VO)_2(TTHA)]_{1.5}\} \cdot 10.5\,H_2O$ **4**

$[Pr_2(H_2O)_6(SO_4)_2][(VO)_2(TTHA)]$ **5**

X-ray crystallographic studies revealed that dimensional variation of oxovanadium(IV)–lanthanide(III) polymers can be realized by exploiting the lanthanide contraction: **1** is an ion-pair complex containing two $[Yb(H_2O)_8]^{3+}$ ions and three $[(VO)_2(TTHA)]^{2-}$ ions per structural formula. In **2** and **3**, lanthanide ions coordinated by seven water molecules are connected to the binuclear $[(VO)_2(TTHA)]^{2-}$ unit through one carboxylic oxygen atom to give a trinuclear cluster. Interestingly, the Eu^{3+} ion is nine-coordinate in **4** with seven water ligands and two bridging oxygen atoms from two $[(VO)_2(TTHA)]^{2-}$ ions, which result in a one-dimensional chain. In **5** the structure is further assembled into a hybrid three-dimensional network with carboxylate and sulfate bridges, in which an interesting framework topology composed of heterometallic V_2Pr_2 and V_4Pr_2 lattices is observed for the first time. With increasing lanthanide atomic radius, the structures of **1**–**5** varied from discrete clusters to three-dimensional networks. At the same time, the lanthanide coordination number increases from eight (Yb, Ho, Gd) to nine (Eu, Pr), and the Ln–O and V···Ln distances increase correspondingly as a result of the lanthanide contraction. The few previous reports on adjusting atomic size for structure modulation are concerned with lanthanide-containing polymers,[7b–d] and as far as we know this is the first example of tuning the structures of 3d–4f complexes by means of the lanthanide-contraction effect.

Results and Discussion

Crystallography: Single-crystal XRD analyses were performed on selected crystals of complexes **1**–**5** (Table 1). Selected bond lengths and angles are listed in Table 2. In polyoxovanadate/metal–ligand systems, organic amines are commonly used as structure-directing agents that act as 1) a charge-compensating and space-filling constituent, 2) a ligand that coordinates to secondary metal sites, and 3) a ligand that directly coordinates to the vanadium skeleton.[5,9] Here the organic acid H_6TTHA was first used as a struc-

Table 1. Crystal data and structure refinement for **1**–**5**.

	1	**2**	**3**	**4**	**5**
formula	$C_{54}H_{146}N_{12}O_{79}V_6Yb_2$	$C_{27}H_{67}HoN_6O_{36.5}V_3$	$C_{27}H_{67}GdN_6O_{36.5}V_3$	$C_{27}H_{71}EuN_6O_{38.5}V_3$	$C_{18}H_{36}N_4O_{28}Pr_2S_2V_2$
M_r	2879.55	1377.62	1369.94	1400.68	1204.33
crystal system	monoclinic	triclinic	triclinic	monoclinic	triclinic
space group	$P2(1)/n$	$P\bar{1}$	$P\bar{1}$	$C2/c$	$P\bar{1}$
crystal size [mm]	$0.20\times0.20\times0.16$	$0.18\times0.14\times0.10$	$0.18\times0.14\times0.10$	$0.35\times0.32\times0.24$	$0.06\times0.08\times0.12$
a [Å]	13.323(4)	10.381(3)	10.395(3)	19.895(7)	6.554(2)
b [Å]	19.741(6)	13.678(4)	13.710(4)	20.127(7)	11.857(4)
c [Å]	21.257(6)	18.954(6)	19.028(6)	26.815(10)	11.933(4)
α [°]	90	83.076(5)	82.935(5)	90	75.523(6)
β [°]	97.326(5)	78.309(5)	78.146(5)	99.000(7)	89.970(7)
γ [°]	90	71.016(4)	71.098(5)	90	75.043(7)
V [Å^3]	5545(3)	2487.8(13)	2506.2(13)	10606(7)	865.4(5)
Z	2	2	2	8	1
ρ_{calcd} [Mg m^{-3}]	1.725	1.839	1.815	1.754	2.311
absorption coefficient [mm^{-1}]	2.269	2.231	1.960	1.790	3.522
$2\theta_{max}$ [°]	52.80	52.84	52.86	52.94	50.06
limiting indices	$-16\le h\le14$	$-12\le h\le12$	$-13\le h\le8$	$-24\le h\le11$	$-7\le h\le7$
	$-24\le k\le24$	$-16\le k\le17$	$-17\le k\le12$	$-24\le k\le25$	$-14\le k\le10$
	$-26\le l\le23$	$-23\le l\le19$	$-23\le l\le22$	$-33\le l\le33$	$-13\le l\le14$
reflections	31575/11321	14400/10066	14469/10135	30241/10863	3620/3047
collected/unique	[R(int) = 0.0423]	[R(int) = 0.0298]	[R(int) = 0.0338]	[R(int) = 0.0914]	[R(int) = 0.0393]
data/restraints/parameters	11321/36/721	10066/36/687	10135/24/677	10863/60/709	3047/0/250
GOF on F^2	1.060	1.055	1.029	1.049	0.961
R_1, wR_2 [$I>2\sigma(I)$]	0.0417, 0.1050	0.0390, 0.0893	0.0462, 0.0945	0.0661, 0.1674	0.0471, 0.0895
R_1, wR_2 (all data)	0.0738, 0.1230	0.0585, 0.1063	0.0786, 0.1157	0.1333, 0.1966	0.0826, 0.1030
largest diff. peak/hole [e Å^{-3}]	0.901/−0.608	1.336/−0.930	1.350/−1.050	0.977/−0.702	1.102/−1.050

Table 2. Selected bond lengths [Å] and angles [°] for **1**–**5**.[a]

Complex **1**									
Yb1−O22	2.269(4)	Yb1−O25	2.274(4)	Yb1−O23	2.358(4)	Yb1−O29	2.272(4)	Yb1−O26	2.302(4)
Yb1−O28	2.368(4)	Yb1−O27	2.374(4)	Yb1−O24	2.381(4)	V1−N1	2.284(4)	V1−O1	1.596(4)
V1−O4	1.992(4)	V1−O6	2.015(4)	V1−O8	1.994(4)	V1−N2	2.164(4)		
O22-Yb1-O29	102.42(19)	O22-Yb1-O25	144.41(16)	O29-Yb1-O25	88.32(15)	O22-Yb1-O26	93.22(19)	O29-Yb1-O26	146.69(15)
O25-Yb1-O26	95.87(15)	O22-Yb1-O23	74.73(17)	O23-Yb1-O27	135.13(15)	O28-Yb1-O27	71.48(13)	O22-Yb1-O24	76.56(17)
O29-Yb1-O24	140.19(14)	O4-V1-O8	87.92(16)	O1-V1-O4	104.70(18)	O1-V1-O8	103.09(19)	O1-V1-O6	95.04(18)
O4-V1-O6	94.83(16)	O8-V1-O6	160.34(15)	O1-V1-N2	100.58(18)	O4-V1-N2	154.03(15)	O8-V1-N2	80.62(15)
Complex **2**									
Ho1−O5	2.304(4)	Ho1−O28	2.318(4)	Ho1−O27	2.333(4)	Ho1−O25	2.356(3)	Ho1−O23	2.359(3)
Ho1−O24	2.359(3)	Ho1−O26	2.397(4)	Ho1−O22	2.410(4)	V1−O1	1.609(4)	V1−O8	1.978(4)
V1−O6	1.996(4)	V1−O4	2.027(4)	V1−N2	2.166(4)	V1−N1	2.294(4)		
O5-Ho1-O28	86.40(14)	O5-Ho1-O27	71.96(15)	O28-Ho1-O27	85.93(16)	O5-Ho1-O25	117.44(14)	O28-Ho1-O25	141.23(13)
O27-Ho1-O25	74.60(15)	O5-Ho1-O23	71.22(13)	O28-Ho1-O23	145.71(13)	O27-Ho1-O23	110.11(15)	O25-Ho1-O23	73.06(12)
O5-Ho1-O24	140.84(14)	O28-Ho1-O24	104.89(14)	O27-Ho1-O24	144.76(14)	O25-Ho1-O24	76.49(13)	O8-V1-O6	87.47(16)
O1-V1-O8	102.88(19)	O1-V1-O6	105.11(18)	O1-V1-O4	96.14(18)	O8-V1-O4	159.69(15)	O6-V1-O4	94.46(15)
O1-V1-N2	100.26(18)	O8-V1-N2	80.37(15)	O6-V1-N2	153.75(16)	O8-V1-N1	84.39(15)	O4-V1-N2	89.38(15)
O1-V1-N1	172.72(18)	O6-V1-N1	75.43(14)	O4-V1-N1	76.59(14)	N2-V1-N1	80.27(15)		
Complex **3**									
Gd1−O28	2.373(4)	Gd1−O27	2.379(5)	Gd1−O25	2.394(4)	Gd1−O23	2.399(4)	Gd1−O26	2.434(4)
Gd1−O22	2.454(4)	Gd1−O24	2.408(4)	V1−O1	1.612(4)	V1−O8	1.978(4)	V1−O6	1.992(4)
V1−O4	2.022(4)	V1−N2	2.175(5)	V1−N1	2.294(5)				
O5-Gd1-O28	86.86(16)	O5-Gd1-O27	71.96(16)	O28-Gd1-O27	85.88(18)	O27-Gd1-O25	74.59(16)	O5-Gd1-O25	117.18(15)
O28-Gd1-O25	141.04(14)	O27-Gd1-O23	110.22(17)	O5-Gd1-O23	70.97(15)	O28-Gd1-O23	145.80(15)	O28-Gd1-O24	105.02(15)
O25-Gd1-O23	73.16(14)	O5-Gd1-O24	140.44(15)	O23-Gd1-O24	79.35(14)	O27-Gd1-O24	144.98(15)	O25-Gd1-O24	76.53(14)
O1-V1-O8	103.1(2)	O5-Gd1-O26	143.38(15)	O8-V1-O6	87.62(18)	O8-V1-O4	159.36(17)	O1-V1-O6	105.3(2)
O1-V1-O4	96.2(2)	O8-V1-N2	80.38(17)	O6-V1-O4	94.40(17)	O1-V1-N2	100.4(2)	O6-V1-N2	153.50(18)
O4-V1-N2	89.04(17)								
Complex **4**									
Eu1−O4	2.373(6)	Eu1−O23	2.392(6)	Eu1−O16	2.405(6)	Eu1−O25	2.409(6)	Eu1−O27	2.413(7)
Eu1−O28	2.451(6)	Eu1−O26	2.456(7)	Eu1−O24	2.518(7)	Eu1−O22	2.728(10)	V1−O1	1.593(6)
V1−O8	1.966(6)	V1−O6	2.002(6)	V1−O5	2.024(6)	V1−N2	2.165(6)	V1−N1	2.295(6)
O4-Eu1-O23	80.7(3)	O4-Eu1-O16	78.8(2)	O23-Eu1-O16	130.3(2)	O4-Eu1-O25	76.0(2)	O23-Eu1-O25	140.3(2)
O16-Eu1-O25	75.8(2)	O4-Eu1-O27	132.9(3)	O23-Eu1-O27	76.7(3)	O16-Eu1-O27	85.3(3)	O25-Eu1-O27	141.6(2)
O4-Eu1-O28	141.4(2)	O23-Eu1-O28	137.9(2)	O16-Eu1-O28	74.0(2)	O25-Eu1-O28	71.2(2)	O27-Eu1-O28	71.5(2)
O1-V1-O8	103.5(3)	O1-V1-O6	104.4(3)	O8-V1-O6	87.1(3)	O1-V1-O5	96.3(3)	O8-V1-O5	159.6(3)
O6-V1-O5	92.9(2)	N2-V1-N1	80.2(2)	O1-V1-N1	172.9(3)	O6-V1-N1	75.1(2)	O5-V1-N2	90.1(2)
O8-V1-N1	83.6(3)	O5-V1-N1	76.7(2)						
Complex **5**									
Pr1−O4#1	2.414(6)	Pr1−O10#2	2.469(6)	Pr1−O6	2.503(6)	Pr1−O14	2.508(5)	Pr1−O2#3	2.514(7)
Pr1−O9	2.534(6)	Pr1−O12	2.534(6)	Pr1−O8	2.581(6)	Pr1−O13	2.597(5)	Pr1−S1	3.171(2)
V1−O5	1.979(6)	V1−O1	2.021(6)	V1−O7	1.587(6)	V1−N2	2.151(7)	V1−N1	2.325(8)
V1−O(3)	2.024(6)								
O4#1-Pr1-O6	72.3(2)	O10#2-Pr1-O6	73.7(2)	O4#1-Pr1-O14	142.60(19)	O10#2-Pr1-O14	82.02(19)	O6-Pr1-O14	136.54(19)
O4#1-Pr1-O2#3	73.4(2)	O10#2-Pr1-O2#3	72.3(2)	O6-Pr1-O2#3	132.2(2)	O14-Pr1-O2#3	69.19(19)	O4#1-Pr1-O9	129.5(2)
O10#2-Pr1-O9	142.3(2)	O6-Pr1-O9	106.2(2)	O9-Pr1-S1	27.64(14)	O12-Pr1-S1	84.73(15)	O8-Pr1-S1	27.27(13)
O13-Pr1-S1	65.36(12)	O7-V1-O1	98.2(3)	O5-V1-O1	158.0(3)	O7-V1-O5	103.9(3)	O7-V1-O3	105.4(3)
O5-V1-O3	84.6(2)	O1-V1-O3	90.0(3)	O7-V1-N2	101.6(3)	O5-V1-N2	81.2(3)		

[a] Symmetry codes: #1: $-x+1,-y+1,-z+1$; #2: $x+1,y,z$; #3: $x,y+1,z$.

ture-directing agent to produce a novel oxovanadium–lanthanide system containing the $[(VO)_2(TTHA)]^{2-}$ unit. In complex **1**, for instance, V1(V2) has a distorted octahedral coordination geometry with three oxygen atoms (V−O 1.992(4)–2.015(4) Å) and one nitrogen atom (V1−N2 2.164(4) Å) from the TTHA ion in the equatorial plane (Figure 1). The terminal oxo atom O1 and N1 occupy the axial positions and form an O1-V1-N1 angle of 171.44(19)°. The V1 atom is displaced from the mean equatorial plane toward the vanadyl oxygen atom by 0.382(3) Å. The V−N distances are clearly in the range observed for a formal V−N single bond,[10] of which the V1−N1 bond length (2.284(4) Å) is modestly elongated due to the *trans*-labilizing influence of the terminal oxo group, as observed in other oxovanadium complexes.[11] In the binuclear $[(VO)_2(TTHA)]^{2-}$ core, the V=O bonds are *cis* to the bridge but *trans* to each other. The two terminal V=O bond lengths of 1.596(4) and 1.600(4) Å are almost identical to the reported mean value of 1.600(1) Å.[12] The V1···V2 distance is 7.479(7) Å.

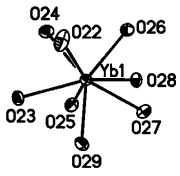

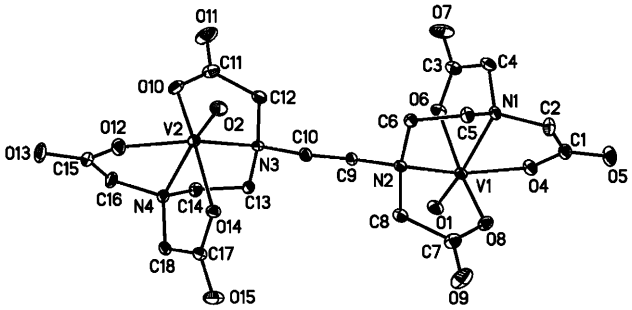

Figure 1. ORTEP plot of $[Yb(H_2O)_8]^{3+}$ ion and $[(VO)_2(TTHA)]^{2-}$ ion in **1**; H atoms and lattice water molecules are omitted for clarity.

Complex **1** crystallizes in the monoclinic system, space group $P2(1)/n$, and is composed of a $[Yb(H_2O)_8]^{3+}$ ion and a $[(VO)_2(TTHA)]^{2-}$ ion (Figure 1). The Yb^{III} atom has a square-antiprismatic coordination geometry formed by eight oxygen atoms from water molecules with an average Yb–O bond length of 2.324(4) Å. The shortest Yb···V distance is 15.885(6) Å.

Complex **2** crystallizes in the triclinic system, space group $P\bar{1}$, and consists of a trinuclear $[Ho(H_2O)_7(VO)_2(TTHA)]^{+}$ ion and a binuclear $[(VO)_2(TTHA)]^{2-}$ ion (Figure 2). The terminal V=O bond lengths vary from 1.605(4) to 1.615(3) Å and compare well with the average value of 1.600(1) Å.[12] The Ho^{3+} ion lies in a square-antiprismatic coordination geometry with O5 of the C1O4O5 group bridging to the V1 ion, and seven coordinated water molecules complete the coordination sphere with an average Ho–O bond length of 2.354(4) Å. The V1···Ho1 distance is 6.068(3) Å. Complex **3** is isomorphous to complex **2** except that the Ho atom is replaced by a Gd atom (Figure 3). The larger atomic radius leads to larger average Gd–O bond length (2.397(4) Å) and V1···Gd1 distance (6.099(4) Å).

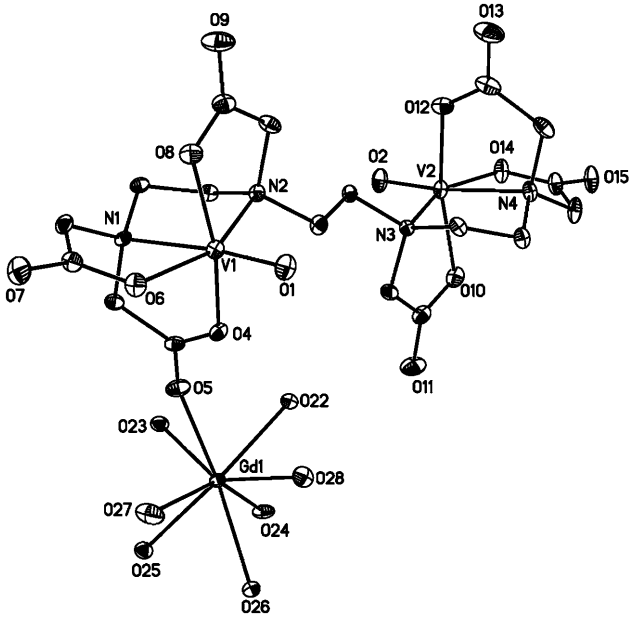

Figure 3. ORTEP plot of $[(VO)_2(TTHA)Gd(H_2O)_7]^{+}$ in **3**; H atoms and lattice water molecules are omitted for clarity.

Complex **4** is a 1D zigzag chain composed of $[(VO)_2(TTHA)]$ building blocks connected by Eu ions (Figure 4). It crystallizes in the monoclinic system, space group $C2/c$. The vanadium ion is 0.398(2) Å from the equatorial plane with respect to the terminal oxo group (V=O 1.593(6) Å). Two oxygen atoms from carboxyl groups and seven coordinated water molecules complete the coordination sphere of the Eu ion, which conforms most closely to a tricapped trigonal prism. The average Eu–O bond length is 2.460(6) Å. The TTHA ion joins two V centers (V1-N2-C9-C10-N3-V2; V1···V2 7.477(5) Å), and the O4C1O5 carboxyl group acts as a $\mu_{1,3}$ bridge connecting the V and Eu centers at a distance of 6.364(7) Å.

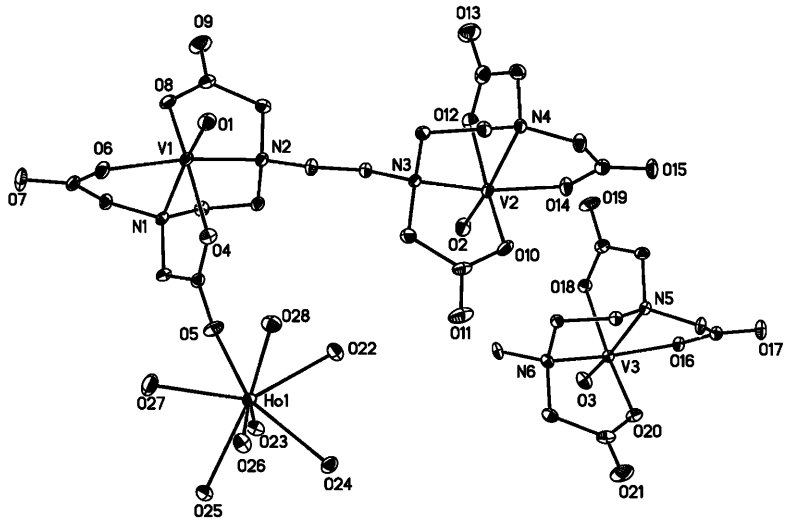

Figure 2. ORTEP plot of $\{[(VO)_2(TTHA)Ho(H_2O)_7][(VO)_2(TTHA)]_{0.5}\}\cdot 8.5H_2O$ (**2**); H atoms and lattice water molecules are omitted for clarity.

Complex **5** crystallizes in the triclinic system, space group $P\bar{1}$, and forms a 3D framework containing nine-coordinate Pr^{3+} centers and six-coordinate V^{4+} centers. The Pr atom is coordi-

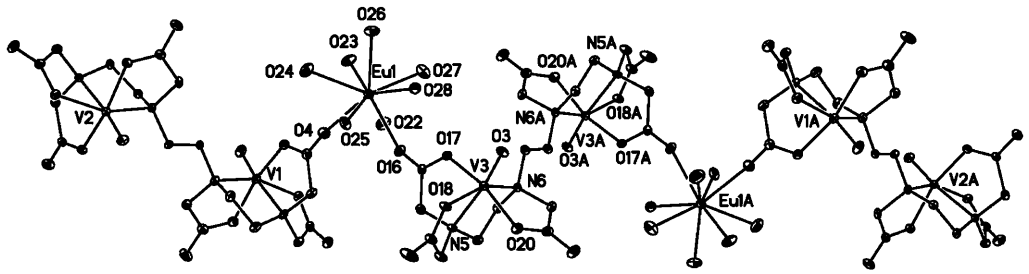

Figure 4. 1D chain of $\{[Eu(H_2O)_7][(VO)_2(TTHA)]_{1.5}\}\cdot 10.5H_2O$ (**4**); H atoms and lattice water molecules are omitted for clarity.

nated by three carboxylic oxygen atoms from TTHA ions, three oxygen atoms from SO_4^{2-} ions, and three water molecules. The coordination geometry around the V^{4+} center is a pseudo-octahedron, in which N1 occupies the *trans* position with respect to the terminal oxo group. The O1, O3, O5, N2 atoms constitute the equatorial plane. The terminal oxo group is *anti* and the vanadium ion is 0.381(6) Å from the equatorial plane with respect to the terminal oxo group. The vanadyl bond length of 1.587(6) Å compares well with the average value of 1.600(1) Å.[12] The Pr and V centers are alternately arrayed and linked by carboxyl groups to construct a heterometallic square lattice V_2Pr_2 with dimensions of 6.377×6.389 Å (Figure 5 a). This lattice composed of 3d and 4f metals, which is extremely rare, assembles into an infinite 1D molecular ladder. The ladders are further linked into 2D layers in the *bc* plane through V–NCCN–V bridges (V–N 2.151(7)–2.325(8) Å) with a V···V distance of 7.540(4) Å to form six-metal V_4Pr_2 rings (Figure 5 a,b). Moreover, along the *a* axis the 2D layers are connected to each other through sulfate bridges with a Pr1–O(SO_4^{2-}) bond length of 2.534(6) Å and a Pr2–O(SO_4^{2-}) bond length of 2.469(6) Å to form a novel 3D framework (Figure 6). The Pr1···Pr2 distance across the sulfate bridge and the Pr1···S1 distance are 6.554(8) and 3.171(2) Å, respectively.[13]

The effect of lanthanide contraction may play an important role in the formation of the structures of the complexes. The lanthanide series can be divided into three groups according to mass: the lighter La–Pm (Group 1), the intermediate Sm–Dy (Group 2), and the heavier Ho–Lu (Group 3). While Group 3 element Yb (**1**) forms an ion-pair complex and Ho and Gd (**2** and **3**) form trinulear structures, the Group 2 element Eu (**4**) gives rise to a one-dimensional chain. However, for Group 1 element Pr (**5**), a three-dimensional network is formed. The structural differences are related to the coordination number of the Ln^{3+} centers, which increases from eight to nine for complexes **1** to **5**. The average bridging Ln–O bond lengths and V···Ln distance increase correspondingly for complexes **1**–**5** (Table 3). All these regular changes result from the decreasing size of these ions.[14]

However, not all structures of 3d–4f complexes show the obvious effect of lanthanide contraction on the structure. Our previous studies on Mn_6Ln_6 coordination polymers gave a series of isomorphous 3d–4f complexes.[2] Because the reaction conditions are similar, the flexibility of the ligand

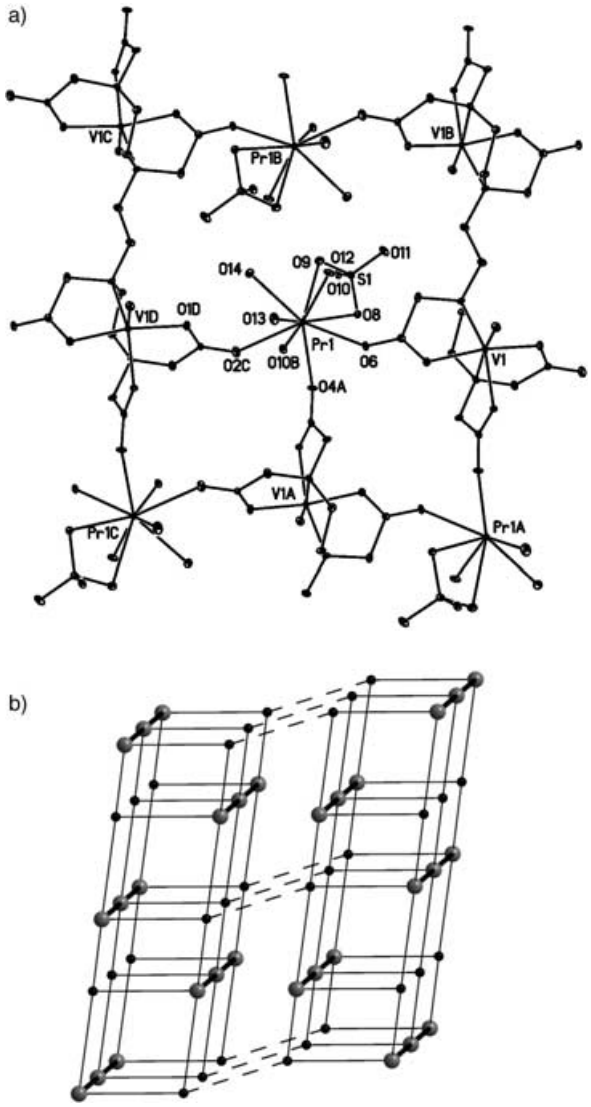

Figure 5. a) V_2Pr_2 and V_4Pr_2 heterometallic lattice of $[Pr_2(H_2O)_6(SO_4)_2][(VO)_2(TTHA)]$ (**5**). b) The 3D framework of complex **5**; V: black; Pr: gray; thin black lines: carboxyl bridges; dashed lines: -NCCN- bridges; thick black lines: sulfate bridges.

may have a strong influence on the variation of the structure dimensionality. H_6TTHA is a large flexible ligand with four nitrogen atoms and twelve oxygen atoms that can coordinate to metal ions, and nine C–C bonds and twelve C–N

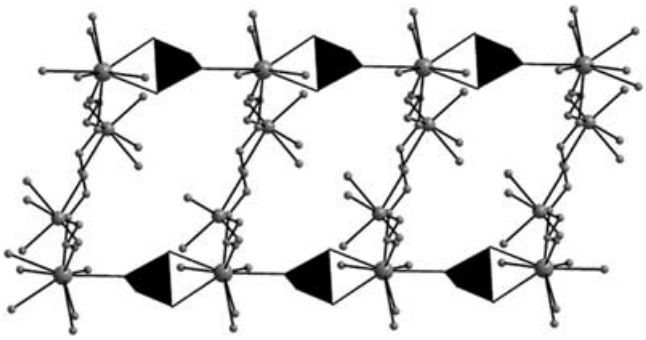

Figure 6. Sulfate bridges in complex **5**. H and part of the C atoms are omitted for clarity.

Table 3. Main structural parameters for **1**–**5**.

	1	**2**	**3**	**4**	**5**
lanthanide ion	Yb	Ho	Gd	Eu	Pr
group by mass	1	1	1	2	3
ionic radius [pm][14]	85.8	89.4	93.8	95.0	101.3
coordination number	8	8	8	9	9
structure dimensionality	ion pair	trinuclear	trinuclear	one-dimensional	three-dimensional
V···V [Å]	7.479(7)	7.459(8)	7.475(6)	7.477(5)	7.540(8)
Ln–O_{av} [Å]	2.324(4)	2.354(4)	2.397(4)	2.460(6)	2.517(1)
Ln···V [Å]	15.885(6)	6.068(3)	6.099(4)	6.364(7)	6.377(7)

bonds can rotate freely around the bond axis. Thus the molecule can easily change its structure to acclimatize itself to the metal ion and form a minimal-energy state. The Mn_6Ln_6 coordination polymers were assembled with pyridine-2,6-dicarboxylic acid (H_2dipic). The greater rigidity of H_2dipic leads to an isostructural series, whereas the flexible H_6TTHA can be influenced by external factors, such as metal-ion radius, to form various dimensional complexes.

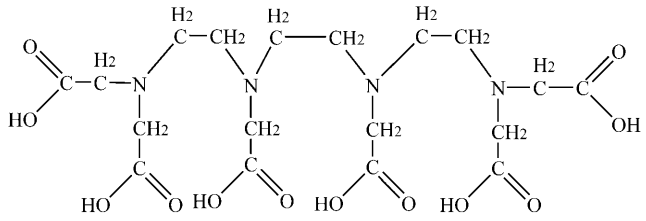

H_6TTHA

IR and UV/Vis spectroscopy: The FTIR spectra of **1**–**5** are similar. All the spectra exhibit a broad band (2900–3700 cm^{-1}), mainly due to $\nu(H_2O)$ centered at about 3430 cm^{-1}. For complex **1**, a very strong band appears at 1636 cm^{-1} due to the antisymmetric stretching of carboxyl groups, and the symmetrical carboxyl stretching band appears at 1385 cm^{-1}. The difference between ν_{as} and ν_s of 252 cm^{-1} is larger than 200 cm^{-1}. This indicates monochelation of the carboxyl group to the metal ion, which is in accord with the X-ray crystal analysis.[15] Another strong band at 971 cm^{-1} is attributed to ν(V=O) stretching.[16] Detailed bands for all complexes are listed in Table 4.

The UV/Vis spectra of complexes **1**–**4** were measured in DMSO solution at a concentration of 10^{-3} M. The absorption spectrum of 3D complex **5** was not recorded due to its extremely low solubility. All complexes exhibit very strong peaks at about 260 nm, which are assignable to charge-transfer transitions in the oxovandium(II) chromophores. Two relatively stronger peaks centered at about 590, 784 nm and a weak shoulder peak around 739 nm were observed that can be attributed to d–d transitions of V^{IV} in an environment close to distorted octahedral. The peaks are red-shifted (by ca. +70 nm) compared to the dinuclear VO–Ln complexes reported by Okawa et al.[16] The hypersensitive transition bands of the lanthanide ions were not observed.[17] The detailed data are listed in Table 4.

Table 4. Primary IR bands and absorption spectra in DMSO Solution of **1**–**5**.

	IR [cm^{-1}]				UV/Vis [nm]			
	$\nu(H_2O)$	ν_{as}(COO)	ν_s(COO)	ν(V=O)	π–π^*	$d_{xy}\rightarrow d_{z^2}$	$d_{xy}\rightarrow d_{x^2-y^2}$	$d_{xy}\rightarrow d_{yz},d_{zx}$
1	3442	1636	1385	972	261	591	739(sh)	784
2	3424	1634	1373	970	260	591	740 (sh)	786
3	3423	1636	1372	971	262	592	739 (sh)	786
4	3425	1632	1371	973	262	591	737 (sh)	784
5	3421	1628	1385	983				

The fluorescence spectrum of complex **4** was also measured in DMSO solution at a concentration of 10^{-3} M. The excitation wavenumber was selected as the maximum of the absorption spectra at 590 and 784 nm, but no emission spectra were observed. This result indicates that the fluorescence of Eu^{III} may be effectively quenched by energy loss from the excited Eu^{III} to the V^{IV} center as intramolecular energy transfer.[16]

Magnetic measurements: Continuous interest has been devoted to the magnetic properties of complexes containing both d and f ions.[18] Since the electronic confirmation of V^{IV} is d^1, the V–Ln complexes constitute an interesting family for the study of exchange coupling. Magnetic measurements on **2**–**5** showed interesting behavior in the temperature range of 2–300 K. The $\chi_M T$ value of 8.14 $cm^3 K mol^{-1}$ of **2** at 300 K is higher than the theoretical value of 7.79 $cm^3 K mol^{-1}$ for 1.5 isolated V^{4+} and 0.5 Ho^{3+} in the $^5I_8$ ground state ($g=5/4$).[19] As the sample is cooled, the $\chi_M T$ value slowly increases and reaches a maximum of 9.84 $cm^3 K mol^{-1}$ at 20 K, and further decreases quickly to

4.10 $cm^3 K mol^{-1}$ at 2 K, which indicates the presence of ferromagnetic interaction in **2** (Figure 7). The χ_M^{-1} verus T plots are almost linear with $C = 8.15$ emu K mol^{-1} and $\theta = 4.79$ K, which confirms the ferromagnetic interactions in **2**. Remarkably, this is the first report of a ferromagnetically coupled

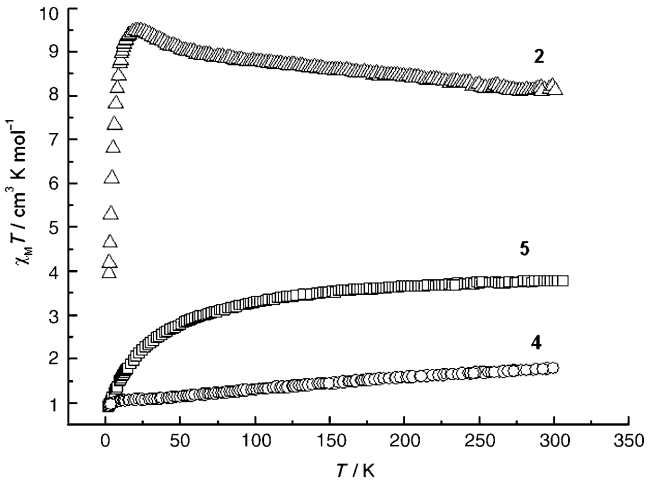

Figure 7. Plots of $\chi_M T$ versus T for **2**, **4**, and **5**.

V–Ln complex. For **4**, the $\chi_M T$ value decreases steadily to 1.06 $cm^3 K mol^{-1}$ on cooling to 10 K, then decreases dramatically to 0.93 $cm^3 K mol^{-1}$ at 2 K. Eu^{3+} has six unpaired electrons and $J = L - S = 0$.[19] The energy levels of the $J = 0$ and $J = 1$ states are very close to each other; therefore, the excited state can easily be achieved by an external magnetic field. The $\chi_M T$ value of **4** at room temperature is 1.78 $cm^3 K mol^{-1}$, which is higher than 1.13 $cm^3 K mol^{-1}$ for three isolated V^{4+} ions. This may be due to the contribution from Eu^{3+} caused by a second-order mixture between the ground state and the excited state. For **5**, the $\chi_M T$ value of 3.78 $cm^3 K mol^{-1}$ at 300 K is lower than the theoretical value of 3.95 $cm^3 K mol^{-1}$ expected for two isolated V^{4+} and two Pr^{3+} in the $^3H_4$ ground state ($g = 4/5$).[20] With decreasing temperature, $\chi_M T$ decreases gradually, then drops rapidly in the lower temperature region to 0.91 $cm^3 K mol^{-1}$ at 2 K. The nature of the magnetic coupling between adjacent V and Ln ions in **4** and **5** could not be interpreted exactly due to the existence of strong spin–orbit coupling for lanthanide atoms.

The magnetic susceptibility of **3** was measured in a field of 1000 Oe. The $\chi_M T$ value at 300 K of 9.57 $cm^3 K mol^{-1}$ is close to the theoretical value of 9.0 $cm^3 K mol^{-1}$ for one free Gd^{3+} and three V^{4+} ions. When the temperature decreases to 30 K the $\chi_M T$ value remains constant, then decreases rapidly on further cooling, possibly due to antiferromagnetic interactions between Gd^{3+} and V^{4+} and/or zero-field splitting (Figure 8). The χ_M^{-1} versus T plots are almost linear with $C = 9.57$ emu K mol^{-1} and $\theta = -0.21$ K. Since Gd^{3+}, with a $^8S_{7/2}$ singlet ground state, does not possess a first-order orbital moment, its magnetic properties are amenable to a rather simple analysis based on a spin-only Hamiltonian.

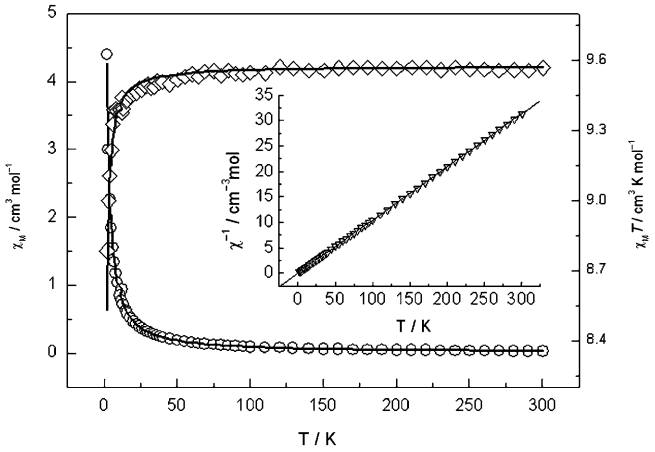

Figure 8. Plots of $\chi_M T$ versus T for **3**. Inset: Fitting to the Curie–Weiss law.

Compared with the carboxyl group between the VO^{2+} and Gd^{3+}, the bridging atom group -N-C-C-N- between two VO^{2+} ions is not an effective pathway for transferring the magnetic interaction, so the total magnetic susceptibility χ_M is given by the sum of the contributions from one half of binuclear anion $[(VO)_2(TTHA)]^{2-}$ and trinuclear cation $[(VO)_2(TTHA)Gd(H_2O)_7]^+$ (composed of mononuclear V and binuclear VGd): $\chi_M = \chi_{VGd} + \chi_V + 0.5\chi_{Bi}$, where χ_{VGd} is given by the expression based on the spin Hamiltonian $\boldsymbol{H} = -\boldsymbol{J}\boldsymbol{S}_{Gd}\cdot\boldsymbol{S}_V$ with the quantum numbers $S_{Gd} = 7/2$ and $S_V = 1/2$ [Eq. (1)][6b].

$$\chi_M = \frac{4Ng^2\beta^2}{kT}\cdot\frac{7 + 15\exp(-4J/kT)}{7 + 9\exp(-4J/kT)} + 2\chi_V \qquad (1)$$

Least-squares fitting of the experimental data leads to $J = -0.21$ cm^{-1}, $g = 1.99$, and the agreement factor R, defined as $R = \Sigma(\chi_{obsd} - \chi_{calcd})^2/(\chi_{obsd})^2$, is 3.8×10^{-5}. The result indicates very weak antiferromagnetic interaction between Gd^{3+} and V^{4+} ions, which may result in the decrease in $\chi_M T$ at low temperature.

EPR spectra: Since the vanadium(IV) ion has a simple $S = 1/2$ electronic spin, and ^{51}V has a high natural abundance and an $I = 7/2$ nuclear spin, the vanadyl ion can be used to assess the bonding of ligands to the divalent complex ion. However, no systematic EPR investigation of V–Ln systems has been carried out. The X-band EPR powder spectra of **1–5** recorded at both room temperature and 77 K show broad bands centered at about $g = 1.98$, except for that of **3**, which is centered at about $g = 2.06$, and the hyperfine pattern can not be resolved. In frozen DMF solution at 77 K, unusual hyperfine structures were observed which are clearly different from those of mononuclear octahedral VO^{2+} complexes.[21] Figure 9 shows the EPR spectrum of **5** with $\langle A \rangle = 68$ G and $\langle g \rangle = 1.98$. Consulting the crystal structures we find that the interaction between vanadium atoms via the -NCCN- bridge is comparatively weak, and the hyperfine

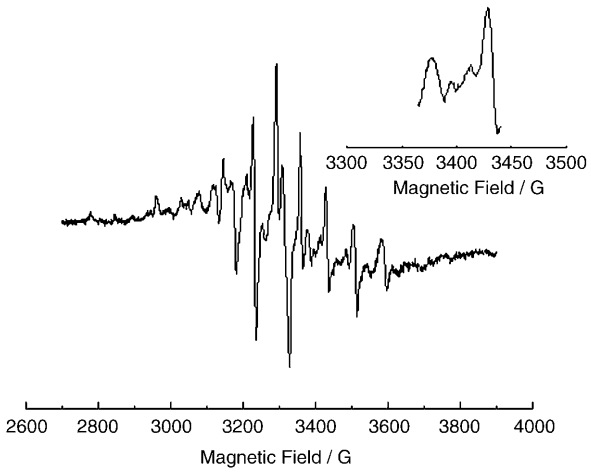

Figure 9. EPR spectrum of **5** recorded at 77 K in DMF solution. Inset: superhyperfine structure of nitrogen atoms

structure may be due to the magnetic spin-exchange interaction between the V^{4+} and Ln^{3+} ions. The superhyperfine structure of nitrogen atoms is also found with an average A value of 16 G.

Conclusion

We have synthesized a new class of 3d–4f complexes. To the best of our knowledge, **4** and **5** are the first V^{IV}–Ln^{III} coordination polymers. The structures vary from trinuclear to 3D with increase of the lanthanide coordination number from eight (Yb, Ho, Gd) to nine (Eu, Pr), and the Ln···O, and the V···Ln distance increases correspondingly as a result of the lanthanide contraction. Notably, **5** has an unprecedented 3D framework. The magnetic behavior of these systems deserves further investigation owing to the need for insights into the fundamental nature of vanadium–lanthanide complexes, to understand the chemistry of such compounds already in use and tailor similar compounds for future applications. Moreover, the successful synthesis of such systems provides an interesting example of using an organic acid as structure-directing agent to construct new oxovanadium(IV) compounds. Given the large variety of bulky organic acids that can be used in this synthetic procedure, and the range of lanthanide elements observed in 3d–4f systems, the scope for further synthesis of other novel oxovanadium(IV)–lanthanide(III) complexes appears to great.

Experimental Section

General remarks: Elemental analyses for C, H, and N were obtained at the Institute of Elemental Organic Chemistry, Nankai University. The FTIR spectra were measured with a Bruker Tensor 27 Spectrometer on KBr disks, and the UV/Vis spectra on a JASCO V-570 Spectrophotometer. The fluorescence spectrum was measured on a Varian Cary Eclipse Fluorescence spectrophotometer. Variable-temperature magnetic susceptibilities were measured on a Quantum Design MPMS-7 SQUID magnetometer. Diamagnetic corrections were made with Pascal's constants for all constituent atoms. The EPR spectra were measured on a BRUKER EMX-6/1 EPR spectrometer.

$[Yb(H_2O)_8]_2[(VO)_2(TTHA)]_3\cdot 21H_2O$ (1): A mixture of H_6TTHA (0.247 g), $VOSO_4\cdot 3H_2O$ (0.109 g), Yb_2O_3 (0.197 g), and H_2O (10 mL) was placed in a 20 mL acid digestion bomb and heated at 150 °C for three days. The product (66 % yield based on V) was collected after washing with water (2×5 mL) and diethyl ether (2×5 mL). Elemental analysis calcd (%) for $C_{54}H_{146}N_{12}O_{79}V_6Yb_2$: C 22.52, H 5.11, N 5.84; found: C 22.87, H 5.29, N 5.41.

$\{[Ho(H_2O)_7(VO)_2(TTHA)][(VO)_2(TTHA)]_{0.5}\}\cdot 8.5H_2O$ (2): A mixture of H_6TTHA (0.247 g), $VOSO_4\cdot 3H_2O$ (0.218 g), Ho_2O_3 (0.378 g), and H_2O (10 mL) was placed in a 20 mL acid digestion bomb and heated at 150 °C for three days. The product (55 % yield based on V) was collected after washing with water (2×5 mL) and diethyl ether (2×5 mL). Elemental analysis calcd (%) for $C_{27}H_{67}HoN_6O_{36.5}V_3$: C 23.54, H 4.90, N 6.10; found: C 23.11, H 4.62, N 5.97.

$\{[Gd(H_2O)_7(VO)_2(TTHA)][(VO)_2(TTHA)]_{0.5}\}\cdot 8.5H_2O$ (3): An aqueous solution of H_6TTHA (25 mL, 0.494 g), $VOSO_4\cdot 3H_2O$ (0.218 g), and Gd_2O_3 (0.363 g) was refluxed for 5 h while stirring, then filtered. Crystals were grown by slow evaporation in ethanol atmosphere. Yield: 45 % based on V. Elemental analysis calcd (%) for $C_{27}H_{67}GdN_6O_{36.5}V_3$: C 23.67, H 4.93, N 6.13; found: C 23.89, H 4.48, N 6.41.

$\{[Eu(H_2O)_7][(VO)_2(TTHA)]_{1.5}\}\cdot 10.5H_2O$ (4): A mixture of H_6TTHA (0.247 g), $VOSO_4\cdot 3H_2O$ (0.109 g), Eu_2O_3 (0.176 g), and H_2O (10 mL) was placed in a 20 mL acid digestion bomb and heated at 150 °C for three days. The product (70 % yield based on V) was collected after washing with water (2×5 mL) and diethyl ether (2×5 mL). Elemental analysis calcd (%) for $C_{27}H_{71}EuN_6O_{38.5}V_3$: C 23.15, H 5.11, N 6.00; found: C 22.91, H 4.77, N 6.15.

$[Pr_2(H_2O)_6(SO_4)_2][(VO)_2(TTHA)]$ (5): A mixture of H_6TTHA (0.247 g), $VOSO_4\cdot 3H_2O$ (0.109 g), $Pr(ClO_4)_3\cdot 6H_2O$, (0.547 g) and H_2O (10 mL) was placed in a 20 mL acid digestion bomb and heated at 150 °C for three days. The product (60 % yield based on V) was collected after washing with water (2×5 mL) and diethyl ether (2×5 mL). Elemental analysis calcd (%) for $C_{18}H_{36}N_4O_{28}Pr_2S_2V_2$: C 17.96, H 3.01, N 4.65; found: C 17.72, H 3.55, N 4.81.

Crystallographic studies: Crystals of **1**–**5** were mounted on glass fibers. Determination of the unit cell and data collection were performed with $Mo_{K\alpha}$ radiation ($\lambda = 0.71073$ Å) on a BRUKER SMART 1000 diffractometer equipped with a CCD camera. The $\omega-\varphi$ scan technique was employed. Crystal parameters and structure refinements for **1**–**5** are summarized in Table 1. Selected bond lengths and angles are listed in Table 2.

The structures were solved primarily by direct methods and secondly by Fourier difference techniques and refined by the full-matrix least-squares method. The computations were performed with the SHELXL-97 program.[22,23] All non-hydrogen atoms were refined anisotropically. The hydrogen atoms were set in calculated positions and refined as riding atoms with a common fixed isotropic thermal parameter.

CCDC-2244535 (**1**), CCDC-227934 (**2**), CCDC-255621 (**3**), CCDC-227933 (**4**), CCDC-227932 (**5**) contain the supplementary crystallographic data for this paper. These data can be obtained free of charge from the Cambridge Crystallographic Data Centre via www.ccdc.cam.ac.uk/data_request/cif.

Acknowledgement

This work was supported by the National Natural Science Foundation of China (Nos. 20425103 and 90101028).

[1] a) J. M. Lehn, *Supramolecular Chemistry*, VCH, Weinheim, **1995**, Chap. 9; b) P. J. Hagrman, D. Hagrman, J. Zubieta, *Angew. Chem.* **1999**, *111*, 2798–2848; *Angew. Chem. Int. Ed.* **1999**, *38*, 2638–2684;

c) M. Albrecht, M. Luta, A. L. Spek, G. van Koten, *Nature* **2000**, *406*, 970–974; d) M. E. Kosal, J.-H. Chou, S. R. Wilson, K. S. Suslick, *Nat. Mater.* **2002**, *1*, 118–121; e) D. Braga, *Chem. Commun.* **2003**, 2751–2754.

[2] a) B. Zhao, P. Cheng, Y. Dai, C. Cheng, D. Z. Liao, S. P. Yan, Z. H. Jiang, G. L. Wang, *Angew. Chem.* **2003**, *115*, 964–966; *Angew. Chem. Int. Ed.* **2003**, *42*, 934–936; b) B. Zhao, P. Cheng, X. Y. Chen, C. Cheng, W. Shi, D. Z. Liao, S. P. Yan, Z. H. Jiang, *J. Am. Chem. Soc.* **2004**, *126*, 3012–3013; c) B. Zhao, X. Y. Chen, P. Cheng, D. Z. Liao, S. P. Yan, Z. H. Jiang, *J. Am. Chem. Soc.* **2004**, *126*, 15394–15395.

[3] a) M. J. Zaworotko, *Chem. Commun.* **2001**, 1–9; b) R. Baggio, M. T. Garland, Y. Moreno, O. Peña, M. Perec, E. Spodine, *J. Chem. Soc. Dalton Trans.* **2000**, 2061–2066.

[4] a) J. T. Rhule, C. L. Hill, D. A. Judd, *Chem. Rev.* **1998**, *98*, 327–358; b) N. Cohen, M. Halberstam, P. Shlimovich, C. J. Chang, H. Shamoon, L. Rossetti, *J. Clin. Invest.* **1995**, *95*, 2501–2509; c) K. H. Thompson, J. H. McNeil, C. Orvig, *Coord. Chem. Rev.* **1999**, *99*, 2561–2572.

[5] a) T. Hirao, *Coord. Chem. Rev.* **2003**, *237*, 1, and references therein; b) B. E. Koene, N. J. Taylor, L. F. Nazar, *Angew. Chem.* **1999**, *111*, 3065–3068; *Angew. Chem. Int. Ed.* **1999**, *38*, 2888–2891; c) D. Hou, K. S. Hagen, C. L. Hill, *J. Am. Chem. Soc.* **1992**, *114*, 5864–5866; d) E. E. Hamilton, P. E. Fanwick, J. J. Wilker, *J. Am. Chem. Soc.* **2002**, *124*, 78–82; e) B. Z. Lin, S. X. Liu, *Chem. Commun.* **2002**, 2126–2127; f) M. J. Manos, A. J. Tasiopoulos, E. J. Tolis, N. Lalioti, J. D. Woollins, A. M. Z. Slawin, M. P. Sigalas, T. A. Kabanos, *Chem. Eur. J.* **2003**, *9*, 695–703; g) A. J. Tasiopoulos, A. N. Troganis, A. Evangelou, C. P. Raptopoulou, A. Terzis, Y. Deligiannakis, T. A. Kabanos, *Chem. Eur. J.* **1999**, *5*, 910–921; h) F. Wolff, C. Lorber, R. Choukroun, B. Donnadieu, *Inorg. Chem.* **2003**, *42*, 7839–7845; i) A. Mukherjee, M. Nethaji, A. R. Chakravarty, *Chem. Commun.* **2003**, 2978–2979.

[6] a) J.-P. Costes, A. Dupuis, J.-P. Laurent, *J. Chem. Soc. Dalton Trans.* **1998**, 735–736; b) J.-P. Costes, F. Dahan, B. Donnadieu, J. Garcia-Tojal, J.-P. Laurent, *Eur. J. Inorg. Chem.* **2001**, 363–365.

[7] a) R. H. Wang, E. Q. Gao, M. C. Hong, S. Gao, J. H. Luo, Z. Z. Lin, L. Han, R. Cao, *Inorg. Chem.* **2003**, *42*, 5468–5470; b) X. F. Li, W. S. Liu, Z. J. Guo, M. Y. Tan, *Inorg. Chem.* **2003**, *42*, 8735–8738; c) L. Pan, X. Y. Huang, J. Li, Y. G. Wu, N. W. Zheng, *Angew. Chem.* **2000**, *112*, 537–540; *Angew. Chem. Int. Ed.* **2000**, *39*, 527–530; d) S. Mizukami, H. Houjou, M. Kanesato, K. Hiratani, *Chem. Eur. J.* **2003**, *9*, 1521–1528.

[8] A. Mondry, P. Starynowicz, *Inorg. Chem.* **1997**, *36*, 1176–1180.

[9] a) Y. Wang, J. Yu, Q. H. Pan, Y. Du, Y. C. Zhou, R. Xu, *Inorg. Chem.* **2004**, *43*, 559–565; b) R. Finn, J. Zubieta, *Chem. Commun.* **2000**, 1321–1322.

[10] W. Yang, C. Lu, *Inorg. Chem.* **2002**, *41*, 5638–5640.

[11] V. Vergopoulos, W. Priebsch, M. Fritzsche, D. Rehder, *Inorg. Chem.* **1993**, *32*, 1844–1849.

[12] D. del Río, A. Galindo, R. Vicente, C. Mealli, A. Ienco, D. Masi, *Dalton Trans.* **2003**, 1813–1820.

[13] A. A. Pinkerton, D. Schwarzenbach, *J. Chem. Soc. Dalton Trans.* **1976**, 2464–2466.

[14] T. Moeller, *The Chemistry of the Lanthanides*, Pergamon Press, Oxford, **1973**.

[15] K. Nakamoto, *Infrared and Raman Spectra of Inorganic and Coordination Compounds*, 4th ed., Wiley, New York, **1986**.

[16] M. Sakmoto, M. Ohsaki, K. Yamamoto, Y. Nakayama, A. Matsumoto, H. Okawa, *Bull. Chem. Soc. Jpn.*, **1992**, 65, 2514–2519.

[17] A. T. Baker, A. M. Hamer, S. E. Livingstore, *Transition Met. Chem.* **1984**, *9*, 423–432.

[18] a) M. Andruh, I. Ramade, E. Codjovi, O. Guillou, O. Kahn, J. C. Trombe, *J. Am. Chem. Soc.* **1993**, *115*, 1822–1829; b) C. Benelli, A. J. Blake, P. E. Y. Milne, J. M. Rawson, R. E. P. Winpenny, *Chem. Eur. J.* **1995**, *1*, 614–618; c) J. P. Costes, F. Dahan, A. Dupuis, *Inorg. Chem.* **2000**, *39*, 165–168.

[19] A. Figuerola, C. Diaz, J. Ribas, V. Tangoulis, J. Granell, F. Lloret, J. Mahía, M. Maestro, *Inorg. Chem.* **2003**, *42*, 641–649.

[20] C. Benelli, D. Gatteshi, *Chem. Rev.* **2002**, *102*, 2369–2387.

[21] S. Samanta, D. Ghosh, S. Mukhopadhyay, A. Endo, T. J. R. Weakley, M. Chaudhury, *Inorg. Chem.* **2003**, *42*, 1508–1517.

[22] G. M. Sheldrick, SHELXS 97, Program for the Solution of Crystal Structures, University of Göttingen, Germany, **1997**.

[23] G. M. Sheldrick, SHELXL 97, Program for the Refinement of Crystal Structures, University of Göttingen: Germany, **1997**.

Received: January 25, 2005
Published online: June 23, 2005

